© 2014. Published by The Company of Biologists Ltd | Development (2014) 141, 3222-3232 doi:10.1242/dev.106229

RESEARCH ARTICLE

Kinesin-II recruits Armadillo and Dishevelled for Wingless signaling in *Drosophila*

Linh Thuong Vuong[1], Bibhash Mukhopadhyay[2] and Kwang-Wook Choi[1,*]

ABSTRACT

Wingless (Wg)/Wnt signaling is fundamental in metazoan development. Armadillo (Arm)/β-catenin and Dishevelled (Dsh) are key components of Wnt signal transduction. Recent studies suggest that intracellular trafficking of Wnt signaling components is important, but underlying mechanisms are not well known. Here, we show that Klp64D, the *Drosophila* homolog of Kif3A kinesin II subunit, is required for Wg signaling by regulating Arm during wing development. Mutations in *klp64D* or RNAi cause wing notching and loss of Wg target gene expression. The wing notching phenotype by Klp64D knockdown is suppressed by activated Arm but not by Dsh, suggesting that Klp64D is required for Arm function. Furthermore, *klp64D* and *arm* mutants show synergistic genetic interaction. Consistent with this genetic interaction, Klp64D directly binds to the Arm repeat domain of Arm and can recruit Dsh in the presence of Arm. Overexpression of Klp64D mutated in the motor domain causes dominant wing notching, indicating the importance of the motor activity. Klp64D shows subcellular localization to intracellular vesicles overlapping with Arm and Dsh. In *klp64D* mutants, Arm is abnormally accumulated in vesicular structures including Golgi, suggesting that intracellular trafficking of Arm is affected. Human KIF3A can also bind β-catenin and rescue *klp64D* RNAi phenotypes. Taken together, we propose that Klp64D is essential for Wg signaling by trafficking of Arm via the formation of a conserved complex with Arm.

KEY WORDS: Armadillo, Dishevelled, *Drosophila* kinesin II, Wingless/Wnt signaling

INTRODUCTION

Wnt signaling plays important roles in growth and patterning. Key protein components involved in canonical Wnt signaling are evolutionarily conserved, and misregulation of this signaling pathway in humans can result in various diseases, including cancer (Clevers, 2006; Coombs et al., 2008). In *Drosophila*, Wg is required for a wide range of processes, such as body patterning in embryos (Bejsovec and Martinez Arias, 1991; DiNardo et al., 1994), growth control and cell fate specification during organogenesis (Siegfried and Perrimon, 1994; Cadigan and Nusse, 1997). Among these, patterning of the embryonic epidermis and the wing imaginal disc has been extensively studied to understand the mechanism of Wg signaling. In embryogenesis, Wg is expressed in a strip of cells within each segmental unit and is required for anterior-posterior patterning of the epidermis (van den Heuvel et al., 1993; Siegfried et al., 1994; McCartney et al., 1999).

[1]Department of Biological Sciences, Graduate School of Nanoscience and Technology, Korea Advanced Institute of Science & Technology, Daejeon 305-701, Korea. [2]MedImmune, Gaithersburg, MD 20878, USA.

*Author for correspondence (kchoi100@kaist.ac.kr)

Received 19 November 2013; Accepted 22 June 2014

In the developing wing disc, Wg is secreted from the dorsoventral (DV) compartment boundary where the wing margin structures are formed (Diaz-Benjumea and Cohen, 1995; Micchelli et al., 1997; Strigini and Cohen, 2000; Baena-Lopez et al., 2012). Wg and Cut expression in the DV boundary are induced by Notch (N) signaling. Wg secretion is known to form a gradient to elicit long-range Wg signaling. Secreted Wg induces the expression of Senseless (Sens) and Distal-less (Dll). Wg can also indirectly induce Cut expression by activating Dl, which in turn activates N in the DV boundary (de Celis and Bray, 1997).

Wg exerts its effects by regulating the transcription of target genes in the responding cells. Arm plays a key role in controlling the transcriptional outputs of the canonical Wg/Wnt pathway (Dierick and Bejsovec, 1999; Stadeli et al., 2006). β-catenin, the vertebrate homolog of Arm, also plays a pivotal role in transducing Wnt signaling in higher animals (Willert and Nusse, 1998). In the absence of a Wg ligand, a protein complex composed of Adenomatous polyposis coli (APC), Axin, GSK3β (Shaggy) and Casein kinase I (Cki) mediates phosphorylation of Arm and directs it for degradation via the proteasome pathway. Binding of Wnt to its receptor Frizzled (Fz) at the cell surface primes a signaling cascade that inhibits the function of this destruction complex via Dishevelled (Dsh), resulting in Arm stabilization. Wg target genes are activated when stabilized Arm enters the nucleus and recruits other coactivators to the target loci through TCF/Pangolin (Pan) (Mosimann et al., 2009). In culture cells, Wnt ligands induce clustering of Fz receptors and Dsh, which in turn promote Axin recruitment and stabilization of β-catenin (Bilic et al., 2007). It has also been proposed that in *Drosophila* embryos, Wg signaling causes relocation of Axin from intracellular vesicles to the plasma membrane, thus inactivating the Axin complex and stabilizing Arm (Cliffe et al., 2003). These studies imply the importance of intracellular trafficking of Wg signaling components for Wnt signaling.

Among the components of the canonical Wg signaling pathway, Arm is unique in that it is not only required for Wg signaling but also for the function of adherens junctions (AJs). Whereas cytosolic Arm is used for transduction of Wg signals, Arm localized at AJs together with α-catenin and cadherin homologs is essential for cell adhesion (Peifer et al., 1993). Arm contains 12 repeated domains in the middle portion of the protein called Arm repeats. The N-terminal region of Arm is crucial for its function at AJs. By contrast, its middle region consisting of the Arm repeat motifs is required for transduction of Wg signaling (Orsulic and Peifer, 1996b), although it is also necessary for proper localization of Arm (Orsulic and Peifer, 1996a; Valenta et al., 2011). Many binding partners for the Arm repeat domain have been found. These partners, including Pan and Cadherin, have overlapping binding sites, suggesting that competition between them might be important for the regulation of Wnt signaling (Pai et al., 1996; Blauwkamp et al., 2008). Despite extensive studies on Arm repeat domain interactions, it is poorly

Development (2014) 141, 3222-3232 doi:10.1242/dev.106229

understood how intracellular trafficking of Arm/β-catenin is regulated. Thus, it is important to identify new partners that could provide clues to the mechanism of intracellular trafficking of Arm/β-catenin for Wnt signaling.

Interestingly, Klp64D, the *Drosophila* homolog of Kif3A of the kinesin II microtubule-based motor (Ray et al., 1999), has been shown to be required for localization of cell junction proteins during morphogenesis of photoreceptor cells in the eye (Mukhopadhyay et al., 2010). Arm is one of the proteins that are mislocalized from AJs in the absence of Klp64D. This raises the possibility that Klp64D might also be required for Wg signaling. Kinesin II motors are typically found as heterotrimeric complexes containing three subunits: two kinesin-like motor subunits, Kif3A and Kif3B, and a non-motor subunit termed Kap3 (Kinesin-associated polypeptide 3) (Cole, 1999; Hirokawa, 2000). *Drosophila* kinesin-II motors are known to be involved in anterograde intraflagellar transport (Tanaka et al., 1998; Ray et al., 1999), but their function in developmental signaling has not been studied. Although mammalian Kif3A has been implicated in the modulation of Wnt signaling (Jimbo et al., 2002; Corbit et al., 2008), it is unknown whether Kif3A and β-catenin play direct roles.

In this study, we show that Klp64D is required for Wg signaling during wing and embryo patterning. Our data indicate that Klp64D is crucial for Arm function by physical interactions and vesicular trafficking. We provide genetic, biochemical and immunocytochemical evidence to support the proposed novel function of the Klp64D-Arm-Dsh complex for Wnt signaling. We also demonstrate similar interaction between human KIF3A and β-catenin. Thus, the function of the kinesin II-β-catenin complex for Wnt signaling might be conserved in higher animals.

RESULTS

Klp64D is required for wing margin development

To test whether Klp64D plays an important role in wing development, we knocked down Klp64D expression in developing flies by targeted expression of double-stranded RNA (dsRNA) for RNA interference (RNAi) using the UAS/Gal4 system (Brand and Perrimon, 1993). First, we used *nubbin (nub)-Gal4* driver, which activates the expression of *klp64D* RNAi in the entire wing pouch of the larval wing disc (Calleja et al., 2000). At 18°C, nearly all animals expressing *klp64D* RNAi induced by *nub-Gal4* (named hereafter *nub>klp64D RNAi*) showed mild defects in the distal part of wings (Fig. 1A,B). Interestingly, most wing defects in this condition were notching in the wing margin and loss of margin bristles, even though *klp64D* RNAi was targeted to all wing pouch cells of the wing disc. As Wg signaling from the DV boundary induces distal outgrowth of wing tissues and sensory organ bristles along the wing margin (Zecca and Struhl, 2010), notching in the wing margin suggests that Klp64D might be preferentially required in the DV boundary region. As Gal4 activity depends on temperature, RNAi effects were stronger at higher temperatures (Brand and Perrimon, 1993). At 29°C, flies with *nub>klp64D RNAi* could almost develop to the adult but died in the pupal case. These flies showed severe shrinkage or complete loss of wing (data not shown), indicating an essential role of Klp64D for wing development.

The defective wing margins described above raised the possibility that Klp64D plays a role in the DV boundary region of the wing disc. To test this hypothesis, we examined the effects of *klp64D* RNAi knockdown targeted to the DV boundary region. *C96-Gal4* was used to induce Gal4 expression at and near the DV boundary that includes both edge and marginal cells (Gustafson and Boulianne, 1996). RNAi knockdown of Klp64D by *C96-Gal4* caused notching along the wing margin in 100% of all tested flies (Fig. 1C,D). However, *C96>klp61F*

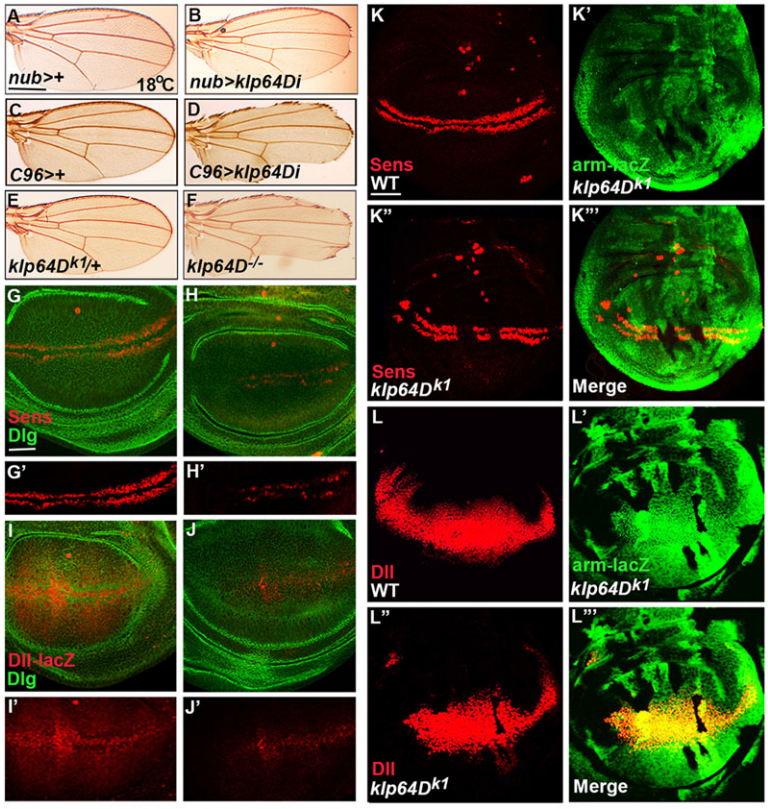

Fig. 1. Klp64D is required for wing margin development and Wg target gene expression. (A,B) Effects of *klp64D* RNAi at 18°C. *nub-Gal4>+* control shows the normal wing (A). *klp64D* RNAi shows notching of the wing margin (B). (C,D) Domain-specific effects of *klp64D* RNAi. (C) *C96-Gal4>+*. (D) *C96>klp64D RNAi* causes notching of the wing margin. (E,F) $klp64D^{k1}$/+ control flies show normal wing (E). Adult wing with $klp64D^{k1}$ clones shows notching phenotype (F). (G,H) Effects of *klp64D* RNAi on Sens expression. (G) *C96-Gal4>+* wing disc showing Sens expression in the DV boundary. (H) *C96-Gal4>klp64D RNAi* results in partial loss of Sens expression. (G′,H′) Red channels of G,H. (I,J) Expression pattern of *Dll-lacZ* in the DV boundary (shown in red). (I) *Dll-lacZ* expression is normal in *C96>+*. (J) *Dll-lacZ* expression is reduced in *C96>klp64Di*. (I′,J′) Red channels of I,J. (K-L‴) Effects of $klp64D^{k1}$ mutant clones in wing disc. Clones were stained for anti-β-gal (green) and either anti-Sens (K-K‴) or anti-Dll (L-L‴) (both red). $klp64D^{k1}$ clones are marked by the absence of *lacZ* activity. Normal expression of Sens and Dll in WT wing discs (K,L). Sens and Dll expression are lost in $klp64D^{k1}$ mutant clones (K‴,L‴). Scale bars: 100 µm (A-F), 50 µm (G-L‴).

Development (2014) 141, 3222-3232 doi:10.1242/dev.106229

RNAi knockdown of a different kinesin family protein, Klp61F, did not affect wing margin development (supplementary material Fig. S1). Independent *klp64D* RNAi lines (see Materials and Methods) gave similar results. To further confirm the effects of *klp64D* RNAi lines, we generated *klp64D*^{k1} null mutant clones in the wing by FLP-mediated mitotic recombination (Xu and Rubin, 1993). Adult wings containing mutant clones showed severe notches (Fig. 1E,F), which is consistent with the *klp64D* RNAi effects on the wing margin.

We then tested whether Klp64D is required for Wg signaling by examining the expression pattern of the Wg target genes *senseless* (*sens*) and *Distal-less* (*Dll*) (Gorfinkiel et al., 1997; Nolo et al., 2000). RNAi knockdown of Klp64D by *C96-Gal4* caused strong reduction in the expression of both Sens and *Dll-lacZ* reporter in the DV boundary region (Fig. 1G-J). We also confirmed that Sens and Dll expression are strongly reduced or lost within *klp64D*^{k1} mutant clones (Fig. 1K‴,L‴). The loss of these markers is unlikely due to cell death at this stage, as cell junction markers were normally expressed (supplementary material Fig. S2). There was also no detectable level of Caspase 3 induction by *klp64D* RNAi targeted to the DV boundary region or to the posterior compartment using *C96-Gal4* or *en-Gal4*, respectively (supplementary material Fig. S3). Furthermore, mutant cells within *klp64D*^{k1} clones showed similar Discs-large (Dlg) membrane marker staining as the wild-type cells outside the clones (supplementary material Fig. S4). Although mutant clones were also found away from the DV boundary (Fig. 1K′,L′), all adult wings with mutant clones showed notching in the wing margin but no loss of wing tissues in non-margin areas (Fig. 1F). As reduced N activity can also cause wing notching, we checked whether *klp64D* mutations might affect N signaling. In contrast to *sens* and *Dll*, the expression of the N target E(spl)m8 was not affected in *klp64D*^{k1} mutant clones (supplementary material Fig. S4). Taken together, these data suggest that Klp64D is preferentially required in the DV boundary region for Wg signaling and wing margin development.

Reduced Klp64D function is suppressed by activated Arm

To identify the functional step of Klp64D in the Wg signaling pathway, we tested whether the *klp64D* RNAi phenotype could be rescued by key components of the pathway. First, we overexpressed the *wg* transgene by *C96-Gal4*. Although Wg was highly expressed (supplementary material Fig. S5), it failed to suppress the notching phenotype of *C96>klp64D RNAi* (Fig. 2F). This suggests that Klp64D is required for Wg signal transduction rather than Wg expression or Wg secretion, as expected from the cell-autonomous phenotype of *klp64D* loss-of-function clones (Fig. 1K-L). We then overexpressed Dsh, but it was also unable to rescue the *klp64D* RNAi phenotype (Fig. 2G). By contrast, overexpression of wild-type Arm or activated Arm (Arm^{S10}) strongly suppressed the *C96>klp64D* RNAi phenotype (Fig. 2H,I), whereas inactive Arm could not (Fig. 2J). Further, benign UAS controls (*UAS-GFP* and *UAS-lacZ*) did not rescue the *klp64D* RNAi phenotype (supplementary material Fig. S6), indicating that the rescue by Arm^{S10} is not due to titration of Gal4 by an extra copy of UAS. The control overexpression of Wg, Dsh or Arm^{S10} on the wild-type background showed little effects on the wing under the same condition (Fig. 2B-D), although *C96>arm*^{S10} has been shown to induce some ectopic hairs at a higher temperature (Helms et al., 1999). These results suggest that Klp64D functions downstream of Wg and is required in a step between Dsh and Arm. Although activated Arm^{S10} strongly suppressed the notching effects of *klp64D* RNAi, wing margin bristles were partially restored in the suppressed wings. Thus, it is possible that in addition to Arm, a full rescue of *klp64D* RNAi effects might require additional factors. Although *C96>Wg* did not cause any detectable phenotypes at 22°C, GFP-Wg overexpression at 25°C led to 100% early pupal lethality without detectable wing development. *klp64D* RNAi was able to partially rescue the lethal effects of GFP-Wg overexpression, resulting in approximately 30% survival of adult flies with small

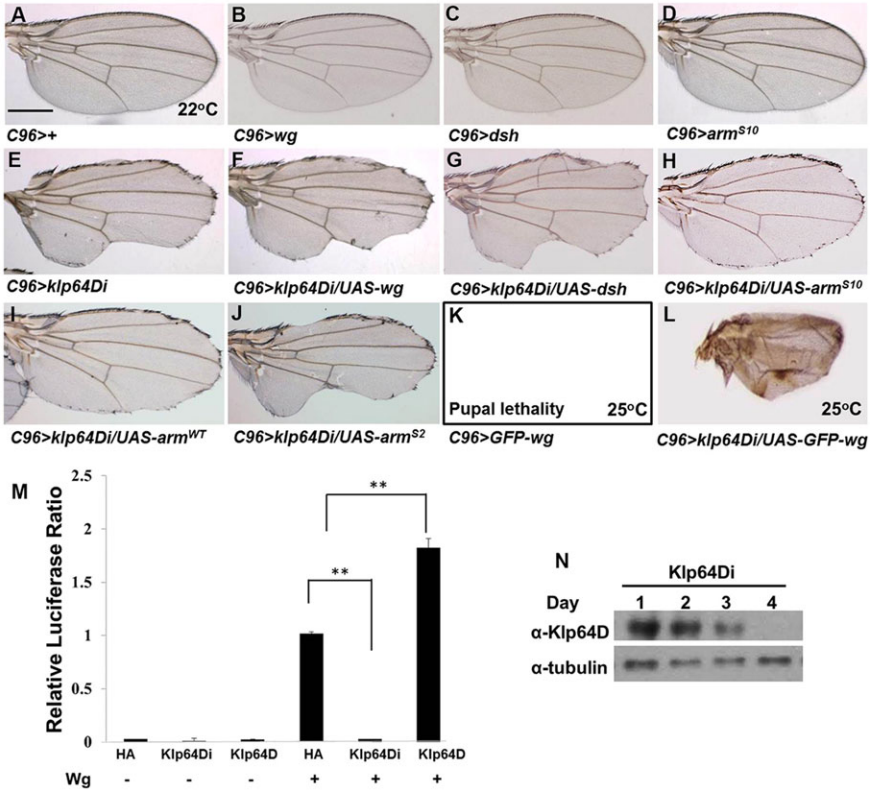

Fig. 2. Klp64D is required for Wg signal transduction. (A-J) Effects of Wg, Dsh and Arm expression on *klp64D* RNAi phenotype. (A) *C96>+* control wing. (B-D) *C96>wg*, *C96>dsh* and *C96>arm*^{S10} show no obvious effect in the wing at 22°C. (E) *C96>klp64D RNAi* shows notches. (F) *C96>klp64D RNAi/UAS-wg*. Wg cannot rescue Klp64D knockdown effect. (G) *C96>klp64D RNAi/UAS-dsh*. Dsh cannot rescue Klp64D knockdown effect. (H-J) *C96>klp64D RNAi/UAS-arm*^{S10} (H), *C96>klp64D RNAi/UAS-arm*^{WT} (I) and *C96>klp64D RNAi/UAS-arm*^{S2} (J). *C96>klp64D RNAi* shows considerable rescue of large wing notches. (J) Arm^{S2} cannot rescue the wing notch phenotype of *C96>klp64D RNAi*. (K,L) Overexpression of GFP-Wg shows pupal lethality at 25°C (K). Klp64D knockdown partially rescues the lethality of GFP-Wg overexpression (L). Klp64D RNAi flies at 25°C show similar wing notching as shown in E. (M) Assay for Wg signaling measured by the relative luciferase ratios in the cells expressing control HA with and without *klp64D* or *klp64D* RNAi, respectively. Wg was added 1 day before cell lysis to induce signaling. Knockdown of Klp64D causes a significant reduction in the luciferase ratio, whereas overexpression of Klp64D increases it (P<0.001). (N) Time course of Klp64D knockdown following RNAi treatment. Cell lysate was loaded into each lane. The blot was probed with anti-Klp64D antibody and anti-α-tubulin. Scale bar: 100 µm.

Development (2014) 141, 3222-3232 doi:10.1242/dev.106229

wings (Fig. 2K,L). This also supports the notion that Klp64D acts downstream of Wg.

To confirm the effect of Klp64D on Wg signaling, a TopFlash assay was performed in *Drosophila* S2 cell culture to measure Wg signaling activity by the ratio of firefly luciferase and *Renilla* luciferase reporter (Beckett et al., 2013). S2 cells transfected with UAS-HA were used as a control in the absence or presence of exogenous Wg secreted in the media. Wg-containing media was added 4 days after transfection to induce signaling. In the absence of Wg, the luciferase ratio was near zero (Fig. 2M). An addition of Wg strongly increased the luciferase ratio to 1.0. This activity was further increased to 1.8 by expressing Klp64D. By contrast, Klp64D knockdown by RNAi (Fig. 2N) inhibited Wg signaling to the basal level (0.008) (Fig. 2M). These results indicate that Wg signaling in S2 cell culture depends on Klp64D. The effects of Klp64D on Wg signaling in S2 cells, where junctional complexes are absent, supports the idea that Klp64D functions on the Wg pathway, rather than having an indirect effect on cell interaction by changing the nature of junctional complexes.

As reduced N activity can cause wing notching, we checked whether *klp64D* mutations might also genetically interact with *N*. Whereas heterozygotes for *N* null ($N^{264\text{-}40}$) or hypomorphic allele (N^{md3}) show small notching in the distal region of the wing margin (Jack and DeLotto, 1992), this phenotype was not enhanced by either $klp64D^{k1}$/+ or arm^{xk22}/+. Besides, overexpression of *N* or the *N* intracellular domain (N^{intra}) could not rescue the phenotype caused by *C96>klp64Di* (supplementary material Fig. S7). These results are consistent with the observation that expression of the N target E(spl)m8 was not affected in $klp64D^{k1}$ mutant clones (supplementary material Fig. S4). Hence, our data support that Klp64D is involved in Wg signaling and is probably independent of the N pathway.

Synergistic genetic interaction between *klp64D* and *arm* mutations

As the *klp64D* RNAi phenotype is suppressed by activated Arm but not by Dsh, the function of Klp64D in the wing appears to be closely related to Arm. We tested this possibility by examining genetic interactions, using mutant alleles or RNAi knockdown of these two genes. Heterozygous flies for arm^{xk22}, a null allele that generates a premature stop codon (Peifer and Wieschaus, 1990), have normal wings (Fig. 3A). However, *nub>klp64D RNAi* knockdown in the arm^{xk22}/+ heterozygote condition resulted in about 27% larger notching than the *nub>klp64D RNAi* control and/or loss of hairs along the posterior margin of the wing (supplementary material Fig. S8), indicating that the reduced *arm* function enhances the *klp64D* knockdown phenotype. A more striking genetic interaction was found between $klp64D^{k1}$/+ and arm^{xk22}/+ heterozygotes. Whereas heterozygous flies for either *arm* or *klp64D* mutation showed normal wings (Fig. 3A,B), more than 50% of double-heterozygous flies (arm^{xk22}/+; $klp64D^{k1}$/+) showed significant loss of wing margin tissue (Fig. 3C).

We then checked whether the genetic interaction between *klp64D* and *arm* mutations affects the expression pattern of Wg target genes, such as *sens* and *Dll*. As expected, wing discs of arm^{xk22}/+; $klp64D^{k1}$/+ double-heterozygotes showed strong reduction or loss of Sens and *Dll-lacZ* expression along the DV boundary region (Fig. 3E,G). This suggests that the wing margin defects shown in arm^{xk22}/+; $klp64D^{k1}$/+ double-heterozygous adult flies were due to defects in Wg signaling.

Wg signaling is also essential for the establishment of segment polarity during embryogenesis (DiNardo et al., 1994; Bauer and Willert, 2012). Loss of Arm or other Wg signaling components causes disruption of the anterior-posterior pattern of denticles in the ventral epidermis of embryo and larva. About 18% of $klp64D^{k33}$ homozygous first instar larvae from $klp64D^{k33}$ heterozygous parents

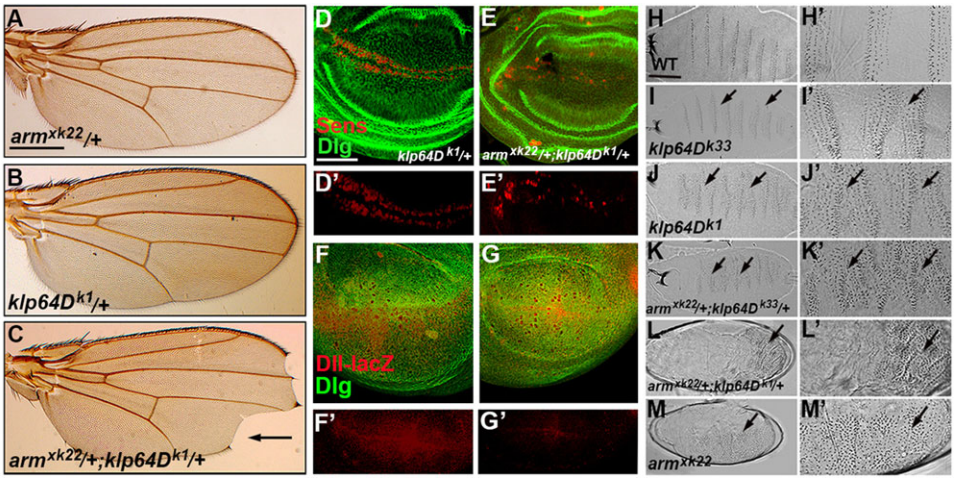

Fig. 3. Genetic interaction between *klp64D* and *arm* mutations. (A-C) Genetic interaction between *klp64D* and *arm*. arm^{xk22}/+ and $klp64D^{k1}$/+ control flies show normal wing (A,B). (C) Double-heterozygotes (arm^{xk22}/+; $klp64D^{k1}$/+) show loss of the wing bristles and notching in the wing, as indicated by arrow. (D,E) Effects of double-heterozygotes (arm^{xk22}/+; $klp64D^{k1}$/+) on Sens expression in the wing disc. (D) *klp64D*/+ heterozygous wing shows normal Sens expression in the DV boundary. (E) Double-heterozygotes (arm^{xk22}/+; $klp64D^{k1}$/+) show partial loss of Sens expression. (D′,E′) Red channels of D,E. (F,G) Effects of double-heterozygotes (arm^{xk22}/+; $klp64D^{k1}$/+) on *Dll-lacZ* expression in the wing disc. (F) $klp64D^{k1}$/+ heterozygotes show normal *Dll-lacZ* expression in the DV boundary. (G) Double-heterozygotes (arm^{xk22}/+; $klp64D^{k1}$/+) result in partial loss of *Dll-lacZ* expression. (F′,G′) Red channels of F,G. (H-J′) *klp64D* is required for embryo patterning and shows genetic interaction with *arm*. (H,H′) Wild-type first instar larvae show the normal anterior-posterior pattern of denticles. (I,I′) $klp64D^{k33}$ mutant shows segment polarity defects in segments A4-7. Arrows indicate the formation of ectopic denticles. (J,J′) $klp64D^{k1}$ larvae show more severe phenotypes than $klp64D^{k33}$ larvae. Ectopic denticles are formed in the space between the normal denticle belts. (K-L′) Genetic interaction of *arm* and *klp64D* mutations. (K,K′) arm^{xk22}/+; $klp64D^{k33}$/+ larvae show more severe ectopic denticles in the space between normal denticle belts than $klp64D^{k33}$ larvae. (L,L′) arm^{xk22}/+; $klp64D^{k1}$/+ embryos at stage 10 show segment polarity phenotype in the posterior region. The anterior region shows loss of cuticle due to incomplete cellularization (Pai et al., 1997). (M,M′) arm^{xk22} mutants show smaller embryos with more severe segment polarity defects. Scale bars: 100 µm (A-C), 50 µm (D-M′).

Development (2014) 141, 3222-3232 doi:10.1242/dev.106229

balanced with *Kr-GFP* marker showed a weak segment polarity phenotype with additional ectopic denticles in the abdominal segments A4-A7 (Fig. 3I,I′; supplementary material Table S1). About 17.7% of null mutant *klp64D*^{k1} embryos showed more severe segment polarity phenotypes than *klp64D*^{k33} (Fig. 3J,J′). To examine the genetic interaction between *arm* and *klp64D*, *arm*^{xk22} and *klp64D* mutant flies were balanced by *FM7 act-GFP* and *TM3 Kr-GFP*, respectively. *arm/+; klp64D/+* double heterozygous flies were recognized by the loss of GFP. About 20% of *klp64D* and *arm* mutations showed synergistic genetic interactions in double-heterozygous embryos (Fig. 3K′,L′; supplementary material Table S1). These data suggest that *klp64D* functions together with *arm* for Wg signaling not only in wing outgrowth but also in segment polarity patterning of the embryo.

Klp64D interacts directly with Arm

Our results for genetic interaction suggest that Klp64D and Arm may physically interact. We carried out biochemical assays to test this possibility of direct interaction. S2 cells were transfected with *Myc-arm* and *Flag-klp64D*. Cell lysates were immunoprecipitated by anti-Flag antibody-conjugated beads and analyzed by western blotting with anti-Myc antibody. In this assay, Arm was co-immunoprecipitated by Klp64D (Fig. 4C). In a similar assay, Klp61F, another kinesin family protein, did not precipitate Arm, supporting the specificity of Klp64D interaction with Arm. The interaction between Klp64D and Arm was also confirmed by co-immunoprecipitation from embryo extracts using either anti-Arm or anti-Klp64D antibody (Fig. 4D). These results indicate that Klp64D and Arm are associated in a protein complex *in vivo*.

To determine whether Klp64D and Arm directly interact in a protein complex, we performed pull-down experiments using purified recombinant GST-fusion proteins. GST-Klp64D fusion protein could pull down Arm (Fig. 4E), indicating direct binding of these two proteins. Next, we examined which regions of Klp64D and Arm proteins are involved in their binding. Kinesin-II consists of a N-terminal motor domain (aa 1-360), a coiled-coil (CC) domain (aa 361-581) and a C-terminal tail domain (aa 582-677) that is used for binding cargos, adaptors and scaffold proteins (Fig. 4B) (Hirokawa et al., 2009). Pull-down assays with truncated Klp64D proteins showed that Arm binds to the CC domain and the tail domain of Klp64D (Fig. 4E).

Arm protein contains a conserved Arm repeat (AR) domain flanked by N- and C-terminal regions (Fig. 4A). To identify the region of Arm involved in binding Klp64D, we tested for binding of Klp64D with three fragments of Arm: the N-terminal fragment (aa 1-140), the Arm repeat region (aa 141-670) and the C-terminal fragment (aa 671-798). These binding assays showed that Klp64D was pulled down by the Arm repeats domain, but not by the N- or C-terminal fragments (Fig. 4F).

Klp64D forms a complex with Dsh and shows functional interaction

As Dsh is required for the inhibition of Arm degradation, we tested whether Klp64D-bound Arm might be physically associated with

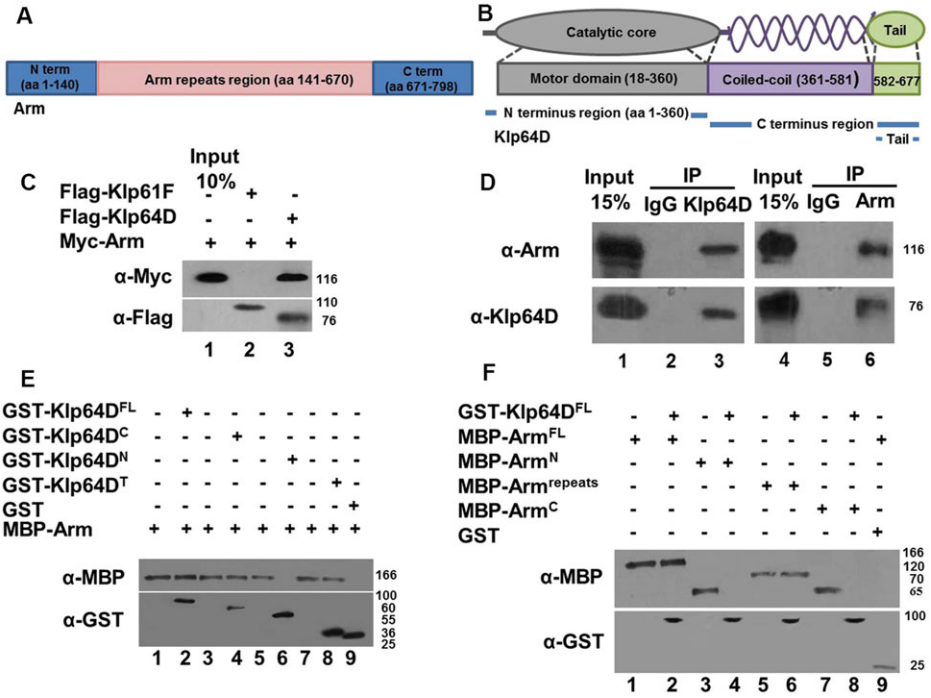

Fig. 4. Klp64D and Arm are directly associated. (A) Domain structure of Arm. (B) Domain structure of *Drosophila* Klp64D. (C) Co-immunoprecipitation of Klp64D and Arm. S2 cells were transfected with *Myc-arm* (input 10%, lane 1) or cotransfected with *Flag-klp61F* and *Myc-arm* (lane 2) or *Flag-klp64D* and *Myc-arm* (lane 3). Cell lysate was immunoprecipitated by anti-Flag antibody-conjugated beads and was analyzed by western blotting. (D) Co-immunoprecipitation assay from embryo lysate. Embryo extracts were immunoprecipitated with anti-Klp64D, anti-Arm or control IgG antibody. The immune complexes and the input (15% of the embryo lysate used in the immunoprecipitation step) were analyzed by immunoblotting with anti-Arm antibody (upper panel, lanes 1-3) or anti-Klp64D antibody (lower panel, lanes 4-6). The same membrane was re-probed to detect Klp64D (lower panel, lanes 1-3) or Arm (upper panel, lanes 4-6). (E) Direct binding of Klp64D and Arm. Lanes 1, 3, 5 and 7 are 10% input of full-length Arm (Arm^{FL}). Pull-down was tried for all Klp64D fragments with GST-full-length Arm (Arm^{FL}), as indicated. All fragments except the N-terminal region of Klp64D (lane 6) and GST alone control (lane 9) show pull-down. (F) Full-length Arm, Arm N-terminal region (Arm^{N}) (1-150), Arm repeats region (151-670) and Arm C-terminal region (Arm^{C}) (671-stop). Lanes 1, 3, 5 and 7 are 15% input. Pull-down was tried for all Arm fragments with GST-Klp64D^{FL} (lanes 2, 4, 6, 8) or GST (lane 9) as indicated. No pull-down is seen in lane 4 (Arm^{N}), lane 8 (Arm^{C}) or lane 9 (GST alone). Molecular weight in kDa indicated in C-F.

Development (2014) 141, 3222-3232 doi:10.1242/dev.106229

Dsh. In pull-down assays, Dsh failed to bind Klp64D (Fig. 5A). However, Dsh was co-immunoprecipitated with both Klp64D full-length protein and the tail domain of Klp64D but not with Klp61F (Fig. 5B). The interaction between Klp64D and Dsh was also confirmed by co-immunoprecipitation from embryo extracts using either anti-Dsh or anti-Klp64D antibody (Fig. 5C). These results indicate that Dsh is indirectly associated with Klp64D in a protein complex. As Dsh does not directly bind to Klp64D, we then tested whether the association of Dsh with Klp64D complex depends on Arm. When the Arm levels were reduced by RNAi knockdown, Klp64D could not associate with Dsh (Fig. 5D,E). We also confirmed that Arm and Dsh form a complex in S2 cells and embryo extracts (Fig. 5F,G). Thus, although Klp64D does not directly bind Dsh, it forms a complex with Dsh in the presence of Arm. Furthermore, *klp64D* and *dsh* mutations showed genetic interaction in a double-heterozygote condition (dsh^{v26}/+; $klp64D^{k1}$/+), resulting in notched wings (Fig. 5I), as seen in arm^{xk22}/+; $klp64D^{k1}$/+ flies (Fig. 3C). These results suggest that the association of Dsh with the Klp64D-Arm complex is important for the Arm function in Wg signaling.

Klp64D shows overlapping subcellular localization with Arm and Dsh

Genetic and physical interactions between Klp64D and Arm raised the possibility that these two proteins might function together in the same

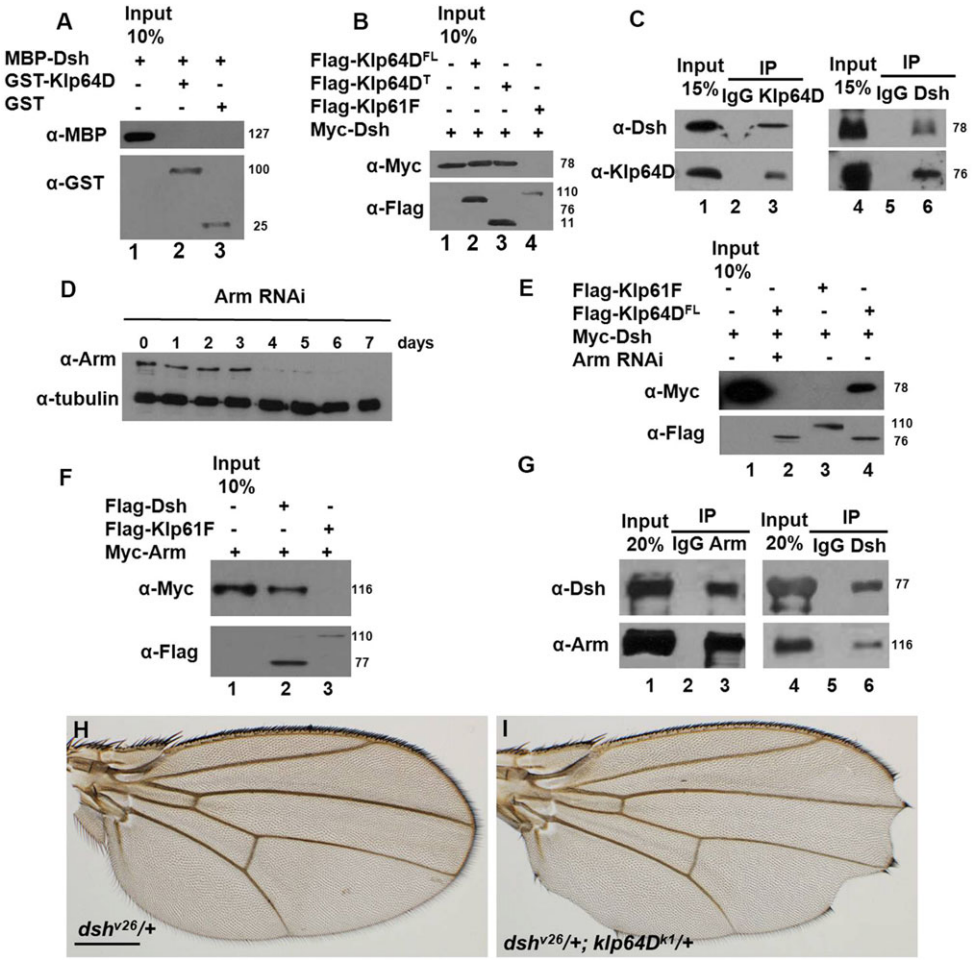

Fig. 5. Interaction between Klp64D and Dsh. (A) Full-length Dsh (Dsh^{FL}) (lane 1, 10% input) was not pulled down by GST-$Klp64D^{FL}$ (lane 2) or GST (lane 3). (B) Co-immunoprecipitation of Klp64D and Dsh. S2 cells were transfected with Myc-Dsh alone (lane 1, 10% input) or cotransfected with Flag-Klp64D (lane 2), Flag-Klp64D tail (lane 3) or Flag-Klp61F (lane 4). Dsh was precipitated with Klp64D (lane 2) and Klp64D tail (lane 3), but not with Klp61F (lane 4). (C) Co-immunoprecipitation assay using embryo lysate. Embryo extracts were immunoprecipitated with anti-Klp64D, anti-Dsh or control IgG antibody. The immune complexes and the input (15% of the embryo lysate used in the immunoprecipitation step) were analyzed by immunoblotting with antibodies specific for Dsh (upper panel, lanes 1-3) or Klp64D (lower panel, lanes 4-6). The same membrane was re-probed to detect Klp64D (lower panel, lanes 1-3) or Dsh (upper panel, lanes 4-6). (D) Time course of Arm knockdown following RNAi treatment. Lysates from approximately 2.5×10^5 cells were loaded into each lane. The blot was probed with anti-Arm and anti-α-tubulin antibodies as a loading control. (E) Co-immunoprecipitation of Klp64D and Dsh after Arm RNAi treatment. S2 cells were transfected with *Myc-dsh* (lane 1) or cotransfected with *Flag-klp64D* and *Myc-dsh* (lanes 2 and 4) or *Flag-klp64F* and *Myc-dsh* (lane 3 as a negative control). Dsh was immunoprecipitated by anti-Flag antibody-conjugated beads and was analyzed by western blotting. Lane 2: Arm RNAi-treated cells; lane 4: no Arm RNAi treatment. (F,G) The interaction between Arm and Dsh. (F) S2 cells were transfected with *Myc-arm* (input 10%, lane 1) or cotransfected with *Flag-dsh* and *Myc-arm* (lane 2) or with *Flag-klp61F* and *Myc-arm* (lane 3). Arm was precipitated with Dsh (lane 2) but not with Klp61F (lane 3). (G) Co-immunoprecipitation assay from embryo lysate. Embryo extracts were immunoprecipitated with anti-Arm, anti-Dsh or control IgG antibody. The immune complexes and the input (20% of the embryo lysate) were analyzed by immunoblotting with anti-Dsh antibody (upper panel, lanes 1-3) or anti-Arm antibody (lower panel, lanes 4-6). The same membrane was re-probed to detect Arm (lower panel, lanes 1-3) or Dsh (upper panel, lanes 4-6). (H,I) Genetic interaction between *klp64D* and *dsh* mutations. (H) dsh^{v26}/+ heterozygous flies show normal wing. (I) Double-heterozygotes (dsh^{v26}/+; $klp64D^{k1}$/+) show loss of the wing bristles and notching in the wing. Scale bar for H,I: 100 µm. Molecular weight in kDa indicated in A-G.

Development (2014) 141, 3222-3232 doi:10.1242/dev.106229

subcellular compartments. To test this possibility, we examined their localizations in tissues. Both an available anti-Klp64D antibody (Baqri et al., 2006) and our newly generated antibodies specifically detected Klp64D protein on a western blot, but could not recognize the protein in tissues by immunocytochemical staining. Thus, we generated a transgenic fly line that carries *UAS-Klp64D-HA* (Hemagglutinin). We then induced expression of *klp64D-HA* using *actin-Gal4* and *nub-Gal4*, and stained with an anti-HA antibody to check the expression pattern of *klp64D* in the embryo and wing imaginal disc. Overexpression by *actin>klp64D-HA* or *nub>klp64D-HA* on the wild-type background did not cause any obvious phenotype. By contrast, Klp64D-HA could rescue the wing phenotype caused by *klp64D* RNAi (supplementary material Fig. S9). Overexpression of Klp64D-HA on *act>klp64D* (or *nub>klp64D*) RNAi background showed a similar level of *klp64D-HA* expression compared with that of control endogenous Klp64D (supplementary material Fig. S9). These data suggest that Klp64D-HA provides sufficient Klp64D function to rescue the RNAi wing phenotype or lethality of the null mutation. Anti-HA staining showed a distribution of Klp64D-HA at cell boundaries in blastoderm embryos. Klp64D-HA staining showed a partially overlapping expression with Arm in the embryo epithelium, suggesting that a fraction of Klp64D localizes to the AJs (Fig. 6A-A″). In the wing disc, Klp64D-HA induced by *nub-Gal4* also showed a significant overlap with Arm at the cell membranes (Fig. 6D-D‴).

In addition to the cell junction staining in the apical region, more basal confocal sectioning of embryo epithelium revealed intracellular puncta co-stained for Arm, Klp64D-HA and Dsh (Fig. 6B-C″). These punctate stainings seem to represent the endogenous pattern of localization, as wild-type embryos stained with anti-Arm and anti-Dsh antibodies also showed similar punctate staining (supplementary material Fig. S10). Similar puncta were also found in wing disc cells (Fig. 6E-E″). Our data indicate that Klp64D and Arm localization partially overlaps in both AJs and intracellular punctate structures in embryo and wing disc cells. In the region basal to AJs of embryonic epithelial cells and wing discs, many Arm and Dsh-GFP puncta were found together, as previously shown (Seto and Bellen, 2004). In the basal region, those puncta were also detected together with Klp64D-HA staining (Fig. 6E-E‴). Furthermore, Klp64D-HA was co-stained with Rab5-YFP, a marker for early endosomes (Fig. 6F-F‴). These results suggest that a significant fraction of Klp64D, Arm and Dsh localize together in the same endosomal compartment. Interestingly, $klp64D^{k1}$ mutant embryos showed abnormally high levels of Arm accumulated in vesicular structures (supplementary material Fig. S11C,D). In normal embryos, only 10% of GM130 puncta overlapped with Arm. However, in *klp64D* mutant embryos, a much higher fraction of GM130 (93%) overlapped with Arm (supplementary material Fig. S11). This trend was also observed in wing discs. In normal wing discs, only a small subset (13%) of GM130 punctate structures overlapped with Arm puncta. By contrast, when Klp64D was reduced in wing discs by RNAi knockdown, the levels of both Arm and GM130 were strongly increased, and GM130 and Arm puncta overlapped significantly (Fig. 7C-D″). This suggests that Arm protein is abnormally accumulated in Golgi when the Klp64D function is compromised.

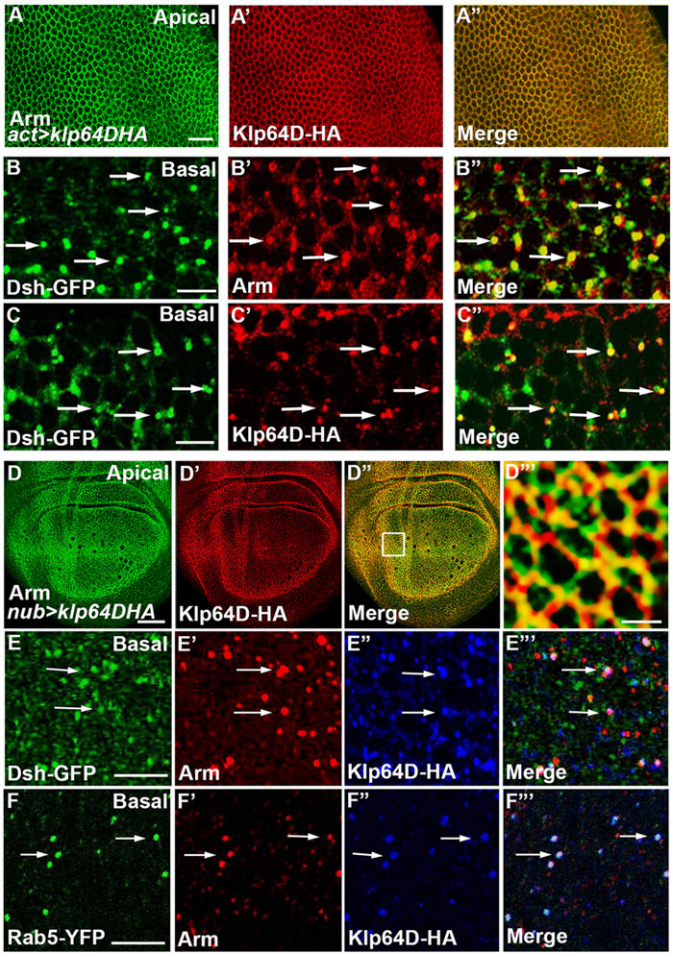

Fig. 6. Overlapping localization of Klp64D-HA, Arm and Dsh. (A-A″) Confocal sections at the level of adherens junctions of embryo epithelium. Embryos were stained for Arm (A) and Klp64D-HA (A′). Merged image (A″) shows a significant overlap between Arm and Klp64D-HA. (B-C″) Basolateral region of embryo epithelium. *cas-DshGFP/act>klp64D-HA* embryos at stage 10 stained for Dsh-GFP (B,C, in green), Arm (B′, in red) and Klp64D-HA (C′, in red). Arrows in B,B′ point to punctate staining of Dsh-GFP overlapping with Arm. Arrows in C,C′ indicate Klp64D-HA protein overlapping with Dsh-GFP. B″ and C″ are merged images of B,B′ and C,C′, respectively. (D-D‴) Confocal sections at the level of AJs. Wing discs were stained for Arm (D) and Klp64D-HA (D′). Klp64D-HA shows localization to the cell membrane together with Arm (D″). D‴ is a higher magnification view of white box in D″. (E-E‴) Basolateral region of wing disc epithelium. *cas-DshGFP/nub>klp64D HA* wing disc stained for Dsh-GFP (E, in green), Arm (E′, in red) and Klp64D-HA (E″, in blue). Arrows indicate punctate staining of Dsh-GFP overlapping with Klp64D-HA and Arm. E‴ is a merged image of E-E″. (F-F‴) Basolateral region of wing disc epithelium. *nub>klp64D HA; Rab5 YFP/+* wing disc stained for Rab5-YFP (F, in green), Klp64D-HA (F′, in red) and Arm (F″, in blue). Arrows indicate punctate staining of Rab5-YFP overlapping with Klp64D-HA and Arm. F‴ is a merge of F-F″. Scale bars: 50 µm.

Motor domain mutants show dominant-negative effects

Protein sequence alignment shows 99% conservation between the motor domains of Klp64D and human KIF3A. It has been shown that mouse kinesin heavy chain proteins mutated in the conserved ATP binding motif can bind microtubules but cannot move (Nakata and Hirokawa, 1995). These rigor type mutants can cause dominant-negative effects. Based on this information, we generated two kinds of defective Klp64D proteins mutated in the identical motor domain (supplementary material Fig. S12A): $Klp64D^{\Delta ABD}$ deleted in eight amino acid core residues for ATP binding (aa 107-114), and $Klp64D^{T114A}$ point mutation at position T114. We tested whether these mutant proteins could show dominant-negative effects in wing discs. Overexpression of wild-type *klp64D* by *C96-Gal4* had no effect on wing development (supplementary material Fig. S12B). On the contrary, overexpression of either $klp64D^{\Delta 107\text{-}114}$ or $klp64D^{T114A}$ resulted in similar notching along the wing margin in

Development (2014) 141, 3222-3232 doi:10.1242/dev.106229

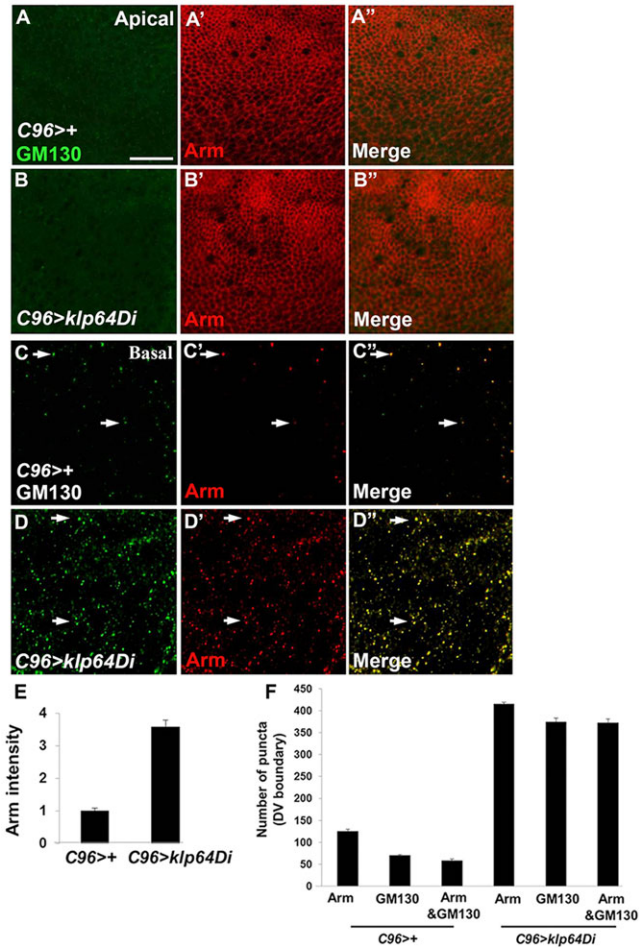

Fig. 7. *klp64D* mutant wing discs show abnormal Arm localization. (A-A″) Apical section of *C96*>+ control wing disc. An apical section of the DV boundary region shows junctional localization of Arm (A′), but little GM130 (A). A″ is a merged image of A and A′. (B-B″) Apical section of *C96>klp64D RNAi* wing disc. An apical section of DV boundary region shows junctional localization of Arm (B′), but little GM130 (B), similar to the wild-type control in A. B″ is a merged image of B and B′. (C-C″) Basal section of *C96*>+ control wing disc. Many GM130 puncta (C, in green) overlap with Arm staining (C′, in red). Arrows in C,C′ point to representative Golgi stainings overlapping with the puncta of Arm. C″ is a merged image of C and C′. (D-D″) Basal section of *C96>klp64D RNAi* wing disc. It shows about fourfold higher levels of punctate Arm overlapping with GM130 puncta. Arrows point to representative puncta of Arm overlapping with GM130 in D,D′. D″ is a merged image of D and D′. Scale bars: 80 µm. (E,F) Quantification of the level and the number of puncta of Arm and GM130 staining in *C96*>+ control and *C96>klp64D RNAi* wing discs. The number of puncta was scored from the DV boundary region shown in this panel.

60% of flies examined (supplementary material Fig. S12D,E). Moreover, the motor domain mutants Klp64D^{T114A} and Klp64D$^{\Delta ABD}$ could not rescue the *C96>klp64Di* phenotype (supplementary material Fig. S12F,G). This dominant notching effect by rigor mutant proteins suggests that the motor activity is required for the normal function of Klp64D in wing margin development.

Human KIF3A binds β-catenin and shows conserved function in *Drosophila*

Klp64D and Arm are conserved homologs of mammalian Kif3A (74% identity) and of β-catenin (72% identity), respectively. To determine whether the interaction between Klp64D and Arm is also conserved, we checked for binding between the mammalian homologs of these two proteins. As shown in Fig. 8, human KIF3A directly interacted with β-catenin in pull-down assays (Fig. 8A). Furthermore, overexpression of human KIF3A fully rescued the wing phenotypes of *C96>klp64D RNAi* (Fig. 8D). Hence, physical and functional interaction between Klp64D and Arm seems to be evolutionarily conserved.

DISCUSSION

Here, we provide evidence for a novel function of Klp64D, the *Drosophila* kinesin II subunit, in wing development. Our genetic analysis suggests that Klp64D is required for Arm function in Wg signaling. This role of Klp64D is supported by synergistic genetic interaction between *klp64D* and *arm* mutations and by physical interaction between Klp64D and Arm. Our data indicate that the *klp64D* RNAi phenotype can be suppressed by activated Arm (Arm^{S10}) but not by inactive Arm. The *klp64D* RNAi phenotype is unlikely due to a defect in *arm* expression, as, based on immunostaining, the level of Arm expression in *klp64D* mutant embryos is not reduced. In fact, *klp64D* mutant embryos show abnormally elevated levels of Arm accumulated in intracellular vesicles (supplementary material Fig. S11). This suggests that Arm is not properly targeted in *klp64D* mutants.

It has been shown in mammalian cells that APC directly binds to the KAP3 non-motor subunit of kinesin II (Jimbo et al., 2002). According to these studies, Wnt-3a not only induces translocation of β-catenin to the nucleus but also to the APC clusters in the membrane protrusions by kinesin II (Jimbo et al., 2002). In our study, we showed a distinct physical interaction between Klp64D and Arm. Given the function of Klp64D as a motor protein, it is possible that Klp64D might be involved in transporting Arm to AJs. As Arm is required for AJ formation and maintenance, loss of Klp64D might impair AJs by failing to transport Arm to the junctions. This is consistent with the disruption of Arm localization in *klp64D* mutant photoreceptor cells (Mukhopadhyay et al., 2010). However, the abnormal junctional localization of Arm in *klp64D* mutant cells might not account for its role in Wnt signaling described in this study, as the junctional function of Arm is probable to be separate from its role in Wnt signaling (Peifer et al., 1993). Furthermore, Fz localized in the apical region is mainly used for planar cell polarity in the wing, whereas canonical Wnt signaling occurs through Fz receptors located in the basal region (Strigini and Cohen, 2000; Wu et al., 2004). Thus, Klp64D function for Wnt signaling might not be directly related to its localization at AJs.

Interestingly, our immunostaining data indicate that Klp64D-HA is not only localized to AJs but also to intracellular punctate structures in the region basal to AJs. Thus, the role of Klp64D in Wg signaling might be related to intracellular trafficking of vesicles containing Arm. It has been shown that some components of Wg signaling, including Arrow (Arr) and Dsh, are internalized to endosomal vesicles (Seto and Bellen, 2006). Upon Wg signaling, Axin relocates from the intracellular vesicles to the plasma membrane, thereby preventing the destruction of Arm (Cliffe et al., 2003). Remarkably, we found that Klp64D-HA staining in the wing disc and embryo epithelia overlaps with Arm and Dsh at a number of intracellular puncta labeled by the early endosomal marker Rab5 (Fig. 6). Furthermore, two kinds of rigor mutant forms of Klp64D cause dominant inhibition of wing margin development, suggesting the importance of the motor activity for endosomal trafficking. As Dsh can form a complex with Klp64D only in the presence of Arm, it appears that Klp64D first binds Arm, and

Development (2014) 141, 3222-3232 doi:10.1242/dev.106229

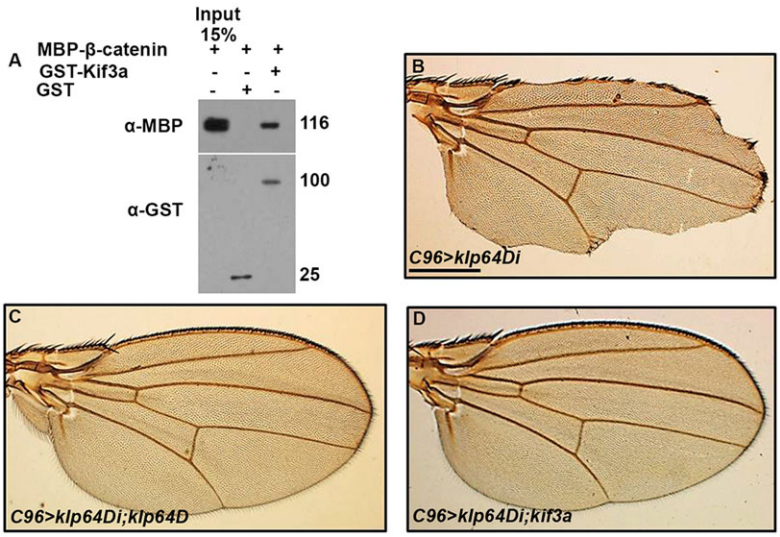

Fig. 8. Human KIF3A can bind β-catenin and function in wing. (A) Direct interaction between human KIF3A and β-catenin. Full-length β-catenin (lane 1, 15% input) was pulled down by GST (lane 2) and GST-Kif3a^{FL} (lane 3). (B) Knockdown of *klp64D* by using *C96-Gal4* causes notching wing phenotype. (C,D) Rescue of *klp64Di* phenotype by Klp64D (C) and human KIF3A (D). Scale bar: 100 µm. Molecular weight in kDa indicated in A.

subsequently Arm might be stabilized, as Dsh is recruited to the Klp64D-Arm complex.

Kinesins are involved in multiple transport pathways, including from the endoplasmic reticulum to Golgi, endosomes and the plasma membrane (Hirokawa and Noda, 2008). Therefore, in the absence of kinesin function, cargo proteins might be mis-targeted or accumulated in vesicles without being transported properly. Indeed, in *klp64D*^{k1} mutant embryos, Arm was found to be abnormally accumulated in intracellular vesicles labeled with GM130 (supplementary material Fig. S11). Similar accumulation of Arm was also found in wing discs when the level of Klp64D was reduced (Fig. 7). In addition, the number of GM130 puncta overlapping with Arm was greatly increased in *klp64D*^{k1} mutant embryos and wing discs, which might be due to an increased processing demand in Golgi (Sengupta and Linstedt, 2011).

It has been suggested that Kif3a in ciliated mammalian cells has a negative role in Wnt signaling by inhibiting Cki phosphorylation of Dvl, thus providing a brake to the Wnt-induced β-catenin stabilization (Corbit et al., 2008). However, this role of cilia and Kif3A in Wnt signaling has not been clearly defined. Recent studies suggest that cilia have no role in Wnt signaling in early development (Goetz and Anderson, 2010). On the contrary, conditional deletion of Kif3A significantly attenuates Wnt signaling in osteoblasts by reducing Wnt-induced accumulation of β-catenin (Qiu et al., 2012), indicating the importance of Kif3A for Wnt signaling. Our study in non-ciliary *Drosophila* wing tissues suggests a novel function of Klp64D in direct trafficking of Arm for Wg signaling. Loss of Klp64D also affects the Wg-dependent anterior-posterior patterning of embryonic segments (Fig. 3). This suggests that Klp64D is an important component of Wg signaling in diverse developmental contexts. We also show that human KIF3A physically interacts with β-catenin and that KIF3A can replace Klp64D *in vivo*. Hence, similar interactions between mammalian kinesin and β-catenin might also play an important role for Wnt signaling in higher animals.

MATERIALS AND METHODS

Genetics

Canton-S was used as the wild-type *Drosophila* strain. UAS lines used were *UAS-klp64D RNAi* [10642R-1 and 10642R-2 from the National Institute of Genetics (NIG), Japan; 45373 and 103358 from the Vienna Drosophila Resource Center, Austria (VDRC)], *UAS-klp61F RNAi* (v52548 and v52559 from VDRC), *UAS-klp64D* (Sarpal et al., 2003), *UAS-arm RNAi* (Bloomington Drosophila Stock Center, USA), *UAS-arm*^{S10} (Pai et al., 1997), *UAS-arm*^{S2} (Kyoto 107878), *UAS-GFP-Wg* (Pfeiffer et al., 2002), *UAS-hid* (Bloomington Drosophila Stock Center) and *UAS-arm*^{Exel} (Bloomington Drosophila Stock Center). Gal4 lines used were *nub-Gal4*, *ptc-Gal4* (Bloomington Drosophila Stock Center) and *C96-Gal4* (Gustafson and Boulianne, 1996).

Transgene construction

Klp64D-HA was cloned into a pUAST vector (Brand and Perrimon, 1993) for the generation of transgenic fly lines.

Generation of mitotic wing clones

Mitotic wing clones were generated by FLP-mediated recombination (Xu and Rubin, 1993). *klp64D*^{k1} *FRT80B/TM6,Tb* flies were crossed into *hsflp; arm-lacZ FRT80B* lines. Wing clones were induced by heat shock at 37°C for 60 min during first and second instar larvae. *klp64D* mutant clones were marked by the absence of *arm-lacZ* expression.

Cuticle preparation and wing mounting

For cuticle preparation, dechorionated embryos were mounted in Hoyer's medium (Gergen and Wieschaus, 1986), incubated at 60°C overnight and viewed with an AxioImager microscope (Zeiss). Wings from adult flies were dissected in isopropanol and mounted in Canada Balsam mounting medium (Gary's Magic Mount) following the protocol of Roberts (Roberts, 1986).

Immunocytochemistry

Wing imaginal discs were dissected from third instar larvae, fixed in 4% paraformaldehyde in PBS and incubated with primary antibodies overnight at 4°C. Embryos were prepared according to a standard method (Foe and Alberts, 1983; Mitchison and Sedat, 1983). More details are described in the supplementary Materials.

Cell culture transfections for TopFlash assay

Drosophila S2R+ cells express all Wg signaling components necessary to respond to exogenously added Wg (Yanagawa et al., 1998). Details of cell transfection and TopFlash assay are described in the supplementary materials.

Immunoprecipitation

Immunoprecipitation from S2 cell lysates and embryos were performed by standard protocols as described in the supplementary materials.

In vitro binding assays

GST pull-down of bacterially expressed proteins was performed by a standard method. Details are described in the supplementary materials.

S2 cell transfection and RNAi

RNAi in S2 cells was carried out with a Megraw protocol (Kao and Megraw, 2004) with minor modifications. More details are described in the supplementary materials.

Quantification of immunostaining

To quantify the Arm protein levels in *klp64D* mutant embryos and the wing disc, and the number of puncta, immunostaining in the embryo and the wing pouch was measured using ImageJ software.

Acknowledgements

We are grateful to Drs Kyung-Ok Cho, Amit Singh and Sang-Chul Nam for crucial comments on the manuscript. We acknowledge the Bloomington Drosophila Stock Center, the Vienna Drosophila RNAi Centre and the Developmental Studies Hybridoma Bank for fly stocks and antibodies. We thank Drs Tadashi Uemura, Hugo Bellen and J. P. Vincent for providing Dsh antibody, Sens antibody and wisir plasmid, respectively.

Competing interests

The authors declare no competing financial interests.

Author contributions

B.M. and K.-W.C. made the initial observation of genetic interaction; L.T.V. and K.-W.C. designed the experiments. L.T.V. performed the experiments;. L.T.V. and K.-W.C. analyzed the data and wrote the paper.

Funding

This research was supported by grants from the World Class University Program [R31-2008-000-10071-0] and a National Research Laboratory grant [NRF-2011-0028326] through the National Research Foundation of Korea, funded by the Korean Ministry of Education, Science & Technology.

Supplementary material

Supplementary material available online at
http://dev.biologists.org/lookup/suppl/doi:10.1242/dev.106229/-/DC1

References

Baena-Lopez, L. A., Nojima, H. and Vincent, J.-P. (2012). Integration of morphogen signalling within the growth regulatory network. *Curr. Opin. Cell Biol.* **24**, 166-172.

Baqri, R., Charan, R., Schimmelpfeng, K., Chavan, S. and Ray, K. (2006). Kinesin-2 differentially regulates the anterograde axonal transports of acetylcholinesterase and choline acetyltransferase in Drosophila. *J. Neurobiol.* **66**, 378-392.

Bauer, M. and Willert, K. (2012). Wnt signaling: the beta-cat(enin)'s meow. *Genes Dev.* **26**, 105-109.

Beckett, K., Monier, S., Palmer, L., Alexandre, C., Green, H., Bonneil, E., Raposo, G., Thibault, P., Le Borgne, R. and Vincent, J. P. (2013). Drosophila S2 cells secrete wingless on exosome-like vesicles but the wingless gradient forms independently of exosomes. *Traffic* **14**, 82-96.

Bejsovec, A. and Martinez Arias, A. (1991). Roles of wingless in patterning the larval epidermis of Drosophila. *Development* **113**, 471-485.

Bilic, J., Huang, Y.-L., Davidson, G., Zimmermann, T., Cruciat, C.-M., Bienz, M. and Niehrs, C. (2007). Wnt induces LRP6 signalosomes and promotes dishevelled-dependent LRP6 phosphorylation. *Science* **316**, 1619-1622.

Blauwkamp, T. A., Chang, M. V. and Cadigan, K. M. (2008). Novel TCF-binding sites specify transcriptional repression by Wnt signalling. *EMBO J.* **27**, 1423-1535.

Brand, A. H. and Perrimon, N. (1993). Targeted gene expression as a means of altering cell fates and generating dominant phenotypes. *Development* **118**, 401-415.

Cadigan, K. M. and Nusse, R. (1997). Wnt signaling: a common theme in animal development. *Genes Dev.* **11**, 3286-3305.

Calleja, M., Herranz, H., Estella, C., Casal, J., Lawrence, P., Simpson, P. and Morata, G. (2000). Generation of medial and lateral dorsal body domains by the pannier gene of Drosophila. *Development* **127**, 3971-3980.

Clevers, H. (2006). Wnt/beta-catenin signaling in development and disease. *Cell* **127**, 469-480.

Cliffe, A., Hamada, F. and Bienz, M. (2003). A role of Dishevelled in relocating Axin to the plasma membrane during wingless signaling. *Curr. Biol.* **13**, 960-966.

Cole, D. G. (1999). Kinesin-II, the heteromeric kinesin. *Cell. Mol. Life Sci.* **56**, 217-226.

Coombs, G. S., Covey, T. M. and Virshup, D. M. (2008). Wnt signaling in development, disease and translational medicine. *Curr. Drug Targets* **9**, 513-531.

Corbit, K. C., Shyer, A. E., Dowdle, W. E., Gaulden, J., Singla, V., Chen, M. H., Chuang, P. T. and Reiter, J. F. (2008). Kif3a constrains beta-catenin-dependent Wnt signalling through dual ciliary and non-ciliary mechanisms. *Nat. Cell Biol.* **10**, 70-76.

de Celis, J. F. and Bray, S. (1997). Feed-back mechanisms affecting Notch activation at the dorsoventral boundary in the Drosophila wing. *Development* **124**, 3241-3251.

Diaz-Benjumea, F. J. and Cohen, S. M. (1995). Serrate signals through Notch to establish a Wingless-dependent organizer at the dorsal/ventral compartment boundary of the Drosophila wing. *Development* **121**, 4215-4225.

Dierick, H. and Bejsovec, A. (1999). Cellular mechanisms of wingless/Wnt signal transduction. *Curr. Top Dev. Biol.* **43**, 153-190.

DiNardo, S., Heemskerk, J., Dougan, S. and O'Farrell, P. H. (1994). The making of a maggot: patterning the Drosophila embryonic epidermis. *Curr. Opin. Genet. Dev.* **4**, 529-534.

Foe, V. E. and Alberts, B. M. (1983). Studies of nuclear and cytoplasmic behaviour during the five mitotic cycles that precede gastrulation in Drosophila embryogenesis. *J. Cell Sci.* **61**, 31-70.

Gergen, J. P. and Wieschaus, E. (1986). Dosage requirements for runt in the segmentation of Drosophila embryos. *Cell* **45**, 289-299.

Goetz, S. C. and Anderson, K. V. (2010). The primary cilium: a signalling centre during vertebrate development. *Nat. Rev. Genet.* **11**, 331-344.

Gorfinkiel, N., Morata, G. and Guerrero, I. (1997). The homeobox gene Distal-less induces ventral appendage development in Drosophila. *Genes Dev.* **11**, 2259-2271.

Gustafson, K. and Boulianne, G. L. (1996). Distinct expression patterns detected within individual tissues by the GAL4 enhancer trap technique. *Genome* **39**, 174-182.

Helms, W., Lee, H., Ammerman, M., Parks, A. L., Muskavitch, M. A. T. and Yedvobnick, B. (1999). Engineered truncations in the Drosophila mastermind protein disrupt Notch pathway function. *Dev. Biol.* **215**, 358-374.

Hirokawa, N. (2000). Stirring up development with the heterotrimeric kinesin KIF3. *Traffic* **1**, 29-34.

Hirokawa, N. and Noda, Y. (2008). Intracellular transport and kinesin superfamily proteins, KIFs: structure, function, and dynamics. *Physiol. Rev.* **88**, 1089-1118.

Hirokawa, N., Noda, Y., Tanaka, Y. and Niwa, S. (2009). Kinesin superfamily motor proteins and intracellular transport. *Nat. Rev. Mol. Cell Biol.* **10**, 682-696.

Jack, J. and DeLotto, Y. (1992). Effect of wing scalloping mutations on cut expression and sense organ differentiation in the Drosophila wing margin. *Genetics* **131**, 353-363.

Jimbo, T., Kawasaki, Y., Koyama, R., Sato, R., Takada, S., Haraguchi, K. and Akiyama, T. (2002). Identification of a link between the tumour suppressor APC and the kinesin superfamily. *Nat. Cell Biol.* **4**, 323-327.

Kao, L. R. and Megraw, T. L. (2004). RNAi in cultured Drosophila cells. *Methods Mol. Biol.* **247**, 443-457.

McCartney, B. M., Dierick, H. A., Kirkpatrick, C., Moline, M. M., Baas, A., Peifer, M. and Bejsovec, A. (1999). Drosophila APC2 is a cytoskeletally-associated protein that regulates wingless signaling in the embryonic epidermis. *J. Cell Biol.* **146**, 1303-1318.

Micchelli, C. A., Rulifson, E. J. and Blair, S. S. (1997). The function and regulation of cut expression on the wing margin of Drosophila: Notch, Wingless and a dominant negative role for Delta and Serrate. *Development* **124**, 1485-1495.

Mitchison, T. J. and Sedat, J. (1983). Localization of antigenic determinants in whole Drosophila embryos. *Dev. Biol.* **99**, 261-264.

Mosimann, C., Hausmann, G. and Basler, K. (2009). Beta-catenin hits chromatin: regulation of Wnt target gene activation. *Nat. Rev. Mol. Cell Biol.* **10**, 276-286.

Mukhopadhyay, B., Nam, S.-C. and Choi, K.-W. (2010). Kinesin II is required for cell survival and adherens junction positioning in Drosophila photoreceptors. *Genesis* **48**, 522-530.

Nakata, T. and Hirokawa, N. (1995). Point mutation of adenosine triphosphate-binding motif generated rigor kinesin that selectively blocks anterograde lysosome membrane transport. *J. Cell Biol.* **131**, 1039-1053.

Nolo, R., Abbott, L. A. and Bellen, H. J. (2000). Senseless, a Zn finger transcription factor, is necessary and sufficient for sensory organ development in Drosophila. *Cell* **102**, 349-362.

Orsulic, S. and Peifer, M. (1996a). An in vivo structure-function study of armadillo, the beta-catenin homologue, reveals both separate and overlapping regions of the protein required for cell adhesion and for wingless signaling. *J. Cell Biol.* **134**, 1283-1300.

Orsulic, S. and Peifer, M. (1996b). Cell-cell signalling: wingless lands at last. *Curr. Biol.* **6**, 1363-1367.

Pai, L.-M., Kirkpatrick, C., Blanton, J., Oda, H., Takeichi, M. and Peifer, M. (1996). Drosophila alpha-catenin and E-cadherin bind to distinct regions of Drosophila Armadillo. *J. Biol. Chem.* **271**, 32411-32420.

Pai, L. M., Orsulic, S., Bejsovec, A. and Peifer, M. (1997). Negative regulation of Armadillo, a Wingless effector in Drosophila. *Development* **124**, 2255-2266.

Peifer, M. and Wieschaus, E. (1990). The segment polarity gene armadillo encodes a functionally modular protein that is the Drosophila homolog of human plakoglobin. *Cell* **63**, 1167-1178.

Peifer, M., Orsulic, S., Pai, L. M. and Loureiro, J. (1993). A model system for cell adhesion and signal transduction in Drosophila. *Development* Suppl. 163-176.

Pfeiffer, S., Ricardo, S., Manneville, J.-B., Alexandre, C. and Vincent, J.-P. (2002). Producing cells retain and recycle Wingless in Drosophila embryos. *Curr. Biol.* **12**, 957-962.
Qiu, N., Xiao, Z., Cao, L., Buechel, M. M., David, V., Roan, E. and Quarles, L. D. (2012). Disruption of Kif3a in osteoblasts results in defective bone formation and osteopenia. *J. Cell Sci.* **125**, 1945-1957.
Ray, K., Perez, S. E., Yang, Z., Xu, J., Ritchings, B. W., Steller, H. and Goldstein, L. S. B. (1999). Kinesin-II is required for axonal transport of choline acetyltransferase in Drosophila. *J. Cell Biol.* **147**, 507-518.
Roberts, D. B. (1986). Basic Drosophila care and techniques. In *Drosophila: A Practical Approach* (ed. D. B. Roberts), pp. 1-38. Washington, DC: IRL Press.
Sarpal, R., Todi, S. V., Sivan-Loukianova, E., Shirolikar, S., Subramanian, N., Raff, E. C., Erickson, J. W., Ray, K. and Eberl, D. F. (2003). Drosophila KAP interacts with the kinesin II motor subunit KLP64D to assemble chordotonal sensory cilia, but not sperm tails. *Curr. Biol.* **13**, 1687-1696.
Sengupta, D. and Linstedt, A. D. (2011). Control of organelle size: the Golgi complex. *Annu. Rev. Cell Dev. Biol.* **27**, 57-77.
Seto, E. S. and Bellen, H. J. (2004). The ins and outs of Wingless signaling. *Trends Cell Biol.* **14**, 45-53.
Seto, E. S. and Bellen, H. J. (2006). Internalization is required for proper Wingless signaling in Drosophila melanogaster. *J. Cell Biol.* **173**, 95-106.
Siegfried, E. and Perrimon, N. (1994). Drosophila wingless: a paradigm for the function and mechanism of Wnt signaling. *Bioessays* **16**, 395-404.
Siegfried, E., Wilder, E. L. and Perrimon, N. (1994). Components of wingless signalling in Drosophila. *Nature* **367**, 76-80.
Städeli, R., Hoffmans, R. and Basler, K. (2006). Transcription under the control of nuclear Arm/beta-catenin. *Curr. Biol.* **16**, R378-R385.
Strigini, M. and Cohen, S. M. (2000). Wingless gradient formation in the Drosophila wing. *Curr. Biol.* **10**, 293-300.
Tanaka, Y., Kanai, Y., Okada, Y., Nonaka, S., Takeda, S., Harada, A. and Hirokawa, N. (1998). Targeted disruption of mouse conventional kinesin heavy chain kif5B, results in abnormal perinuclear clustering of mitochondria. *Cell* **93**, 1147-1158.
Valenta, T., Gay, M., Steiner, S., Draganova, K., Zemke, M., Hoffmans, R., Cinelli, P., Aguet, M., Sommer, L. and Basler, K. (2011). Probing transcription-specific outputs of beta-catenin in vivo. *Genes Dev.* **25**, 2631-2643.
van den Heuvel, M., Klingensmith, J., Perrimon, N. and Nusse, R. (1993). Cell patterning in the Drosophila segment: engrailed and wingless antigen distributions in segment polarity mutant embryos. *Development* Suppl. 105-114.
Willert, K. and Nusse, R. (1998). Beta-catenin: a key mediator of Wnt signaling. *Curr. Opin. Genet. Dev.* **8**, 95-102.
Wu, J., Klein, T. J. and Mlodzik, M. (2004). Subcellular localization of frizzled receptors, mediated by their cytoplasmic tails, regulates signaling pathway specificity. *PLoS Biol.* **2**, E158.
Xu, T. and Rubin, G. M. (1993). Analysis of genetic mosaics in developing and adult Drosophila tissues. *Development* **117**, 1223-1237.
Yanagawa, S., Lee, J.-S. and Ishimoto, A. (1998). Identification and characterization of a novel line of Drosophila Schneider S2 cells that respond to wingless signaling. *J. Biol. Chem.* **273**, 32353-32359.
Zecca, M. and Struhl, G. (2010). A feed-forward circuit linking wingless, fat-dachsous signaling, and the warts-hippo pathway to Drosophila wing growth. *PLoS Biol.* **8**, e1000386.